THE JOURNAL OF BIOLOGICAL CHEMISTRY VOL. 285, NO. 10, pp. 7127–7134, March 5, 2010

DIP2A Functions as a FSTL1 Receptor*[S]

Received for publication, September 23, 2009, and in revised form, December 21, 2009 Published, JBC Papers in Press, January 6, 2010, DOI 10.1074/jbc.M109.069468

Noriyuki Ouchi, Yasuhide Asaumi, Koji Ohashi, Akiko Higuchi, Saki Sono-Romanelli, Yuichi Oshima, and Kenneth Walsh[1]

From the Molecular Cardiology/Whitaker Cardiovascular Institute, Boston University School of Medicine, Boston, Massachusetts 02118

FSTL1 is an extracellular glycoprotein whose functional significance in physiological and pathological processes is incompletely understood. Recently, we have shown that FSTL1 acts as a muscle-derived secreted factor that is up-regulated by Akt activation and ischemic stress and that FSTL1 exerts favorable actions on the heart and vasculature. Here, we sought to identify the receptor that mediates the cellular actions of FSTL1. We identified DIP2A as a novel FSTL1-binding partner from the membrane fraction of endothelial cells. Co-immunoprecipitation assays revealed a direct physical interaction between FSTL1 and DIP2A. DIP2A was present on the cell surface of endothelial cells, and knockdown of DIP2A by small interfering RNA reduced the binding of FSTL1 to cells. In cultured endothelial cells, knockdown of DIP2A by small interfering RNA diminished FSTL1-stimulated survival, migration, and differentiation into network structures and inhibited FSTL1-induced Akt phosphorylation. In cultured cardiac myocytes, ablation of DIP2A reduced the protective actions of FSTL1 on hypoxia/reoxygenation-induced apoptosis and suppressed FSTL1-induced Akt phosphorylation. These data indicate that DIP2A functions as a novel receptor that mediates the cardiovascular protective effects of FSTL1.

FSTL1 (follistatin-like 1; also referred to TSC36) is a secreted extracellular glycoprotein that was initially identified from a mouse osteoblast cell line as a transforming growth factor-β (TGF-β)[2]-regulated gene (1). Prior studies have shown that FSTL1 can have antiproliferative effects on cells (2, 3) and that it can exert anti-inflammatory (4, 5) or pro-inflammatory (6) actions in animal models. Recently, we have found that FSTL1 is up-regulated in the myocardium in response to Akt1-induced hypertrophic growth and myocardial stress, including pressure overload, ischemia-reperfusion, and myocardial infarction (7). Systemic delivery of FSTL1 protects the heart from ischemia-reperfusion injury in mice, which is accompanied by reduced myocyte apoptosis. More recently, we have shown that FSTL1 is up-regulated and secreted in skeletal muscle in response to Akt-mediated growth and ischemic injury (8). FSTL1 promotes endothelial cell function *in vitro* and accelerates ischemia-induced revascularization *in vivo*. Thus, we proposed that FSTL1 functions as an injury-induced secreted protein that protects against ischemic damage. However, the molecular mechanisms by which FSTL1 promotes cardiovascular cell protection and function are incompletely understood.

FSTL1 possesses extracellular calcium-binding and follistatin-like domains and is categorized as the follistatin family member of proteins (9). Other members of the follistatin family act through their ability to function as extracellular binding partners of TGF-β superfamily proteins and antagonize the binding of these ligands to the receptors (10). However, it has never been documented that FSTL1 modulates cell function by binding members of the TGF-β superfamily, as do follistatin and FSTL3 (11). In this regard, FSTL1 has relatively low protein sequence homology to follistatin (16%) and FSTL3 (15%), whereas follistatin and FSTL3 display a 32% identity (7). Furthermore, we have found that the administration of FSTL1 elicits the rapid activation of intracellular signaling molecules in cells that are incubated in low-mitogen media (7, 8). Thus, we do not favor the notion that FSTL1 acts indirectly on cells through its ability to inhibit the actions of TGF-β superfamily proteins. In this study, we sought to identify the cell-surface receptor of FSTL1 that mediates the direct actions of FSTL1 on signaling and phenotype in endothelial cells and cardiac myocytes. Our observations indicate that DIP2A (Disco-interacting protein 2 homolog A) serves as a novel cell-surface receptor that is required for the functional response of cardiovascular cells to FSTL1.

EXPERIMENTAL PROCEDURES

Materials—Anti-phospho-Akt (Ser^{473}) and anti-Akt antibodies were purchased from Cell Signaling Technology. Anti-tubulin antibody was purchased from Oncogene. Anti-mouse FSTL1 antibody was obtained from R&D Systems. Anti-human DIP2A antibody was obtained from Abcam. Anti-FLAG M2 affinity gel was purchased from Sigma.

Preparation of Recombinant Mouse FSTL1 Protein—Full-length mouse *Fstl1* cDNA tagged with FLAG at the C terminus, which lacks the signal peptide, was obtained by PCR and subcloned into the pMIB/V5-His insect cell expression vector (Invitrogen) containing honeybee melittin secretion signal for protein secretion. This vector was transfected into insect Sf9 cells, and a stable cell line was generated by blasticidin selec-

* This work was supported, in whole or in part, by National Institutes of Health Grants HL77774, HL86785, AG15052, and HL81587 (to K. W.). This work was also supported by grants from Banyu Life Science Foundation International (to Y. A.).

[S] The on-line version of this article (available at http://www.jbc.org) contains supplemental Fig. 1.

[1] To whom correspondence should be addressed: Molecular Cardiology/Whitaker Cardiovascular Inst., Boston University School of Medicine, 715 Albany St., W611, Boston, MA 02118. Tel.: 617-414-2390; Fax: 617-414-2391; E-mail: kxwalsh@bu.edu.

[2] The abbreviations used are: TGF-β, transforming growth factor-β; HUVEC, human umbilical vein endothelial cell; siRNA, small interfering RNA; Ad, adenovirus; NRVM, neonatal rat ventricular myocyte; MALDI, matrix-assisted laser desorption/ionization.

tion. The culture supernatants were collected, and FLAG-FSTL1 was allowed to bind anti-FLAG M2 affinity gel. FLAG-FSTL1 was eluted by incubation with 3×FLAG peptide and subsequently dialyzed against phosphate-buffered saline for use in all experiments.

Cell Culture and Western Blot Analysis—Human umbilical vein endothelial cells (HUVECs) were cultured in endothelial cell growth medium-2 (Lonza) (12). For gene knockdown experiments, the small interfering RNAs (siRNAs) targeting human DIP2A was purchased from Dharmacon (ON-TARGET*plus* SMARTpool). HUVECs were transfected with 40 nM each siRNA using Lipofectamine 2000 reagent (Invitrogen) (13). Control cultures were transfected with unrelated siRNAs (ON-TARGET*plus* non-targeting pool, Dharmacon). In some experiments, siRNA-transfected HUVECs were treated with FSTL1 protein or vehicle in endothelial cell basal medium-2 (Lonza) without serum for the indicated lengths of time. In some experiments, siRNA-transfected HUVECs were infected with adenoviral constructs encoding mouse *Fstl1* (Ad-FSTL1) (8) or β-galactosidase (Ad-β-galactosidase) at a multiplicity of infection of 10 for 8 h and placed in serum-free endothelial cell basal medium-2 for the indicated lengths of time.

Neonatal rat ventricular myocytes (NRVMs) were cultured as described previously (14). NRVMs were transfected with 40 nM of siRNAs targeting rat DIP2A or unrelated siRNAs (ON-TARGET*plus* SMARTpool or ON-TARGET*plus* non-targeting pool) using Lipofectamine 2000 reagent (7). In some experiments, siRNA-transfected NRVMs were transduced with Ad-FSTL1 (8) or Ad-β-galactosidase at a multiplicity of infection of 50 for 16 h and placed in serum-free Dulbecco's modified Eagle's medium for the indicated lengths of time.

Cell lysates were resolved by SDS-PAGE. The membranes were immunoblotted with the indicated antibodies at 1:1000 dilution, followed by the secondary antibody conjugated with horseradish peroxidase at 1:5000 dilution. An ECL Western blotting detection kit (Amersham Biosciences) was used for detection.

Analysis of FSTL1-binding Protein—The membrane fractions of HUVECs were isolated using a cell fraction system (Bio-Vision) according to the manufacturer's instructions. Membrane fractions were incubated with FLAG-FSTL1 (2 μg/ml) or vehicle for 2 h, precipitated with anti-FLAG M2 affinity gel, and separated by electrophoresis on denaturing SDS-4–15% polyacrylamide gels. Proteins were stained with carrier-complexed silver, and the candidate band was excised and digested with trypsin. Tryptic peptides were analyzed by MALDI mass spectrometry using a Voyager-DE™ STR system (Applied Biosystems) (15). Peptide mass fingerprints were analyzed using the NCBI Database. In some experiments, the proteins were transferred to membranes, and immunoblot analysis was performed with anti-DIP2A or anti-FSTL1 antibody.

Cloning of Full-length Human DIP2A—Full-length human *DIP2A* cDNA (GenBank™ accession number NM_015151) was obtained by PCR using cDNA produced from RNA that was isolated from HUVECs and then subcloned into the pcDNA3.1/V5-His mammalian cell expression vector (Invitrogen), which expresses human DIP2A as a fusion to a His epitope at the C terminus. The DIP2A-expressing pcDNA3.1/V5-His vector was transfected into COS-7 cells using Lipofectamine 2000. After cells were incubated for 48 h, the cell lysates were collected. Cells transfected with empty vectors (mock) were used as a negative control. For pulldown assays, cell lysates were treated with FSTL1 protein or vehicle for 1 h, precipitated with MagneHis particles (Promega), and subjected to SDS-PAGE.

Detection of Cell-surface DIP2A—Cells were treated with anti-DIP2A antibody (mouse IgG, 5 μg/ml) or normal mouse IgG for 60 min, stained with Alexa Fluor® 488-conjugated anti-mouse IgG (Invitrogen), and analyzed by flow cytometric analysis (FACScan). To determine the localization of DIP2A in HUVECs, immunocytochemical analysis was performed. Cells were fixed with 4% paraformaldehyde in phosphate-buffered saline and washed with phosphate-buffered saline. After blocking with phosphate-buffered saline containing 5% fetal bovine serum, cells were incubated with anti-DIP2A antibody (2.5 μg/ml), followed by incubation with Alexa Fluor® 594-conjugated anti-mouse IgG (Invitrogen). The cells were mounted using VECTASHIELD® mounting medium containing 4′,6-diamidino-2-phenylindole (Vector Laboratories). Cells were observed with a Nikon deconvolution wide-field epifluorescence microscope system.

Binding of FSTL1 to Endothelial Cells—FSTL1 binding to the cell surface was determined by enzyme-linked immunosorbent assay. HUVECs were incubated with the indicated concentrations of biotinylated recombinant FSTL1 (NHS-Biotin, Pierce) for 60 min and treated with streptavidin-conjugated horseradish peroxidase, followed by incubation with QuantaBlu fluorogenic peroxidase substrate (Pierce). Fluorescence intensity was measured with a fluorescence microplate reader (SpectraMax). The data were represented by subtracting nonspecific binding in the presence of a 100-fold excess of unlabeled FSTL1 from the total binding.

Determination of DIP2A mRNA—After transfection with siRNAs for 48 h, total RNA was isolated from HUVECs or NRVMs using an RNeasy micro kit (Qiagen). cDNA was produced using ThermoScript RT-PCR systems (Invitrogen). Quantitative real-time PCR was performed on an iCycler iQ real-time PCR detection system (Bio-Rad) using SYBR Green I (Applied Biosystems) as a double-stranded DNA-specific dye according to the manufacturer's instructions as described previously (16). The primers were 5′-GGTGAACCTGTCATGTGTGC-3′ and 5′-CAGGTCCTTGAAGAGCTTGG-3′ for human DIP2A; 5′-GCTCCAAGCAGATGCAGCA-3′ and 5′-CCGGATGTGAGGCAGCAG-3′ for human 36B4; 5′-TAGTGACCCTGTAATGTTTATGGTT-3′ and 5′-CATCCTTTCTCGTTAATGGTACTTC-3′ for rat DIP2A; and 5′-TCACCACCATGGAGAAGGC-3′ and 5′-GCTAAGCAGTTGGTGGTGCA-3′ for rat glyceraldehyde-3-phosphate dehydrogenase. DIP2A expression levels are presented relative to 36B4 or glyceraldehyde-3-phosphate dehydrogenase levels.

Analysis of Endothelial Cell Differentiation, Viability, and Migration—The formation of network structures by HUVECs on growth factor-reduced Matrigel (BD Biosciences) was performed as described previously (12). Twenty-four-well culture plates were coated with Matrigel according to the manufacturer's instructions. HUVECs were seeded on coated plates at 5×10^4 cells/well in serum-free endothelial cell basal medium-2

and incubated at 37 °C for 18 h. The degree of network formation was quantified by measuring the areas of tubes in three randomly chosen fields from each well using NIH Image software. Cell viability was measured with methanethiosulfonate reagent using the CellTiter 96 AQ_{ueous} kit (Promega) according to the manufacturer's instructions (17). Migratory activity was measured using a modified Boyden chamber assay as described previously (8).

Assessment of Apoptosis—We determined cardiomyocyte and HUVEC apoptosis by measuring the extent of nucleosome fragmentation using a cell death detection kit (Roche Applied Science). After transfection with siRNAs, NRVMs were transduced with Ad-FSTL1 or Ad-β-galactosidase at a multiplicity of infection of 50 and exposed to 12 h of hypoxia and 24 h of reoxygenation (hypoxia/reoxygenation) to induce apoptosis. Hypoxia was generated using a GasPak system (BD Biosciences) as described previously (7, 18). After transfection with siRNAs, HUVECs were infected with Ad-FSTL1 or Ad-β-galactosidase at a multiplicity of infection of 10 for 8 h and placed in serum-free endothelial cell basal medium-2 for 48 h. At least eight samples were analyzed for each experimental group.

Statistical Analysis—All data are expressed as means ± S.E. Differences were analyzed by Student's unpaired *t* test or analysis of variance for multiple comparisons. A level of $p < 0.05$ was accepted as statistically significant.

RESULTS

Association between DIP2A and FSTL1—To identify FSTL1-binding proteins in the membrane of endothelial cells, crude membrane fractions from HUVECs were incubated with or without FLAG-tagged FSTL1 protein, precipitated with FLAG affinity gel, and subjected to SDS-PAGE. We detected one unique protein band at 170 kDa in membrane fractions treated with FLAG-FSTL1, but not in those without FLAG-FSTL1, as assessed by silver staining (Fig. 1*A*). This region of the SDS-polyacrylamide gel was excised, digested with trypsin, and analyzed by MALDI mass spectrometry. Analysis of the peptide mass fingerprint using the NCBI Database revealed that 40 peptide masses correspond to the protein DIP2A and comprise 30% of its total sequence (supplemental Fig. 1). DIP2A is the human homolog of the *Drosophila* protein referred to as DIP2 (Disco-interacting protein 2).

To test whether DIP2A is detected in FLAG-precipitated material from the FLAG-FSTL1-treated membrane fraction of HUVECs, DIP2A protein expression was assessed by Western blot analysis. DIP2A was detected in the membrane fraction that was incubated with FLAG-tagged FSTL1, but not in its absence (Fig. 1*B*). To further investigate the association of FSTL1 with DIP2A, COS-7 cells were transfected with plasmid containing the cDNA for human DIP2A fused to a polyhistidine sequence at the C terminus (DIP2A-His). DIP2A protein was detected in the nickel resin-precipitated fraction only when COS-7 cells were transfected with DIP2A-His (Fig. 1*C*). Cell lysates from DIP2A-His-transfected COS-7 were incubated with FSTL1 protein or vehicle and precipitated with nickel resin, followed by Western immunoblot analysis with anti-FSTL1 antibody. FSTL1 protein was detected only in the nickel resin-precipitated material from the lysates of DIP2A-His-transfected COS-7 that were incubated with recombinant FSTL1 protein (Fig. 1*C*).

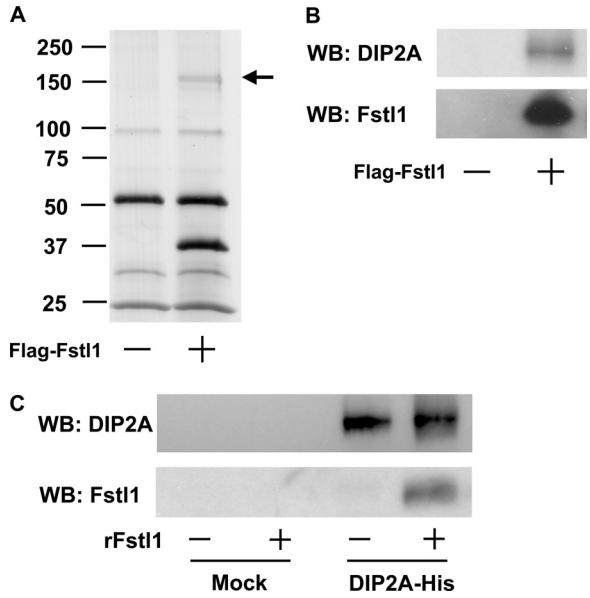

FIGURE 1. **Interaction of FSTL1 with a novel binding protein, DIP2A.** *A*, detection of FSTL1-binding protein in membrane fractions of HUVECs. Membrane fractions were incubated in the presence or absence of FLAG-FSTL1 protein (2 μg/ml) and then immunoprecipitated with anti-FLAG affinity gel, followed by SDS-PAGE. Proteins were stained with carrier-complexed silver. The *arrow* indicates possible binding protein partners of FSTL1. *B*, DIP2A is immunoprecipitated by FLAG-FSTL1 from HUVEC membranes. Immunoprecipitated material was subjected to SDS-PAGE, followed by Western blot (*WB*) analysis with anti-DIP2A and anti-FSTL1 antibodies. *C*, FSTL1 is immunoprecipitated with nickel resin when DIP2A-His is present in the cell lysates. COS-7 cells were transfected with DIP2A-His or mock-transfected. Cell lysates were incubated in the presence or absence of recombinant FSTL1 protein (*rFstl1*; 400 ng) for 1 h and then subjected to immunoprecipitation with nickel resin. Immunoprecipitated material was subjected to SDS-PAGE, and Western blot analysis was performed with anti-DIP2A and anti-FSTL1 antibodies.

Analysis of the DIP2A subcellular localization by PSORT II software predicted that its highest probability of subcellular localization is the plasma membrane (43.5%). Thus, experiments were performed to detect DIP2A on the cell surface. HUVECs were incubated with anti-DIP2A antibody or control mouse IgG and stained with fluorescence-conjugated anti-mouse IgG. FACScan analysis detected the expression of DIP2A on the cell surface (Fig. 2*A*). Immunocytochemical analysis also revealed that the fluorescence signal for DIP2A was observed at the cell periphery of HUVECs (Fig. 2*B*). Experiments were also performed to test whether DIP2A expression is required for the binding of FSTL1 to intact endothelial cells. Transfection of HUVECs with siRNA against human DIP2A reduced DIP2A expression by 66.1 ± 4.8% compared with unrelated siRNA (Fig. 2*C*). Biotinylated FSTL1 protein bound to HUVECs in a saturable manner (Fig. 2*D*). Half-maximal binding was observed at the approximate concentration of 37 ng/ml biotinylated FSTL1. Knockdown of DIP2A with siRNA led to a reduction of the binding of biotinylated FSTL1 to HUVECs compared with control siRNA treatment (Fig. 2*D*).

Role of DIP2A in Endothelial Cell Responses to FSTL1—We have shown previously that FSTL1 promotes endothelial cell survival, migration, and differentiation into network structures (8). To test the role of DIP2A in FSTL1-stimulated endothelial cell survival, HUVECs were transduced with siRNA targeting

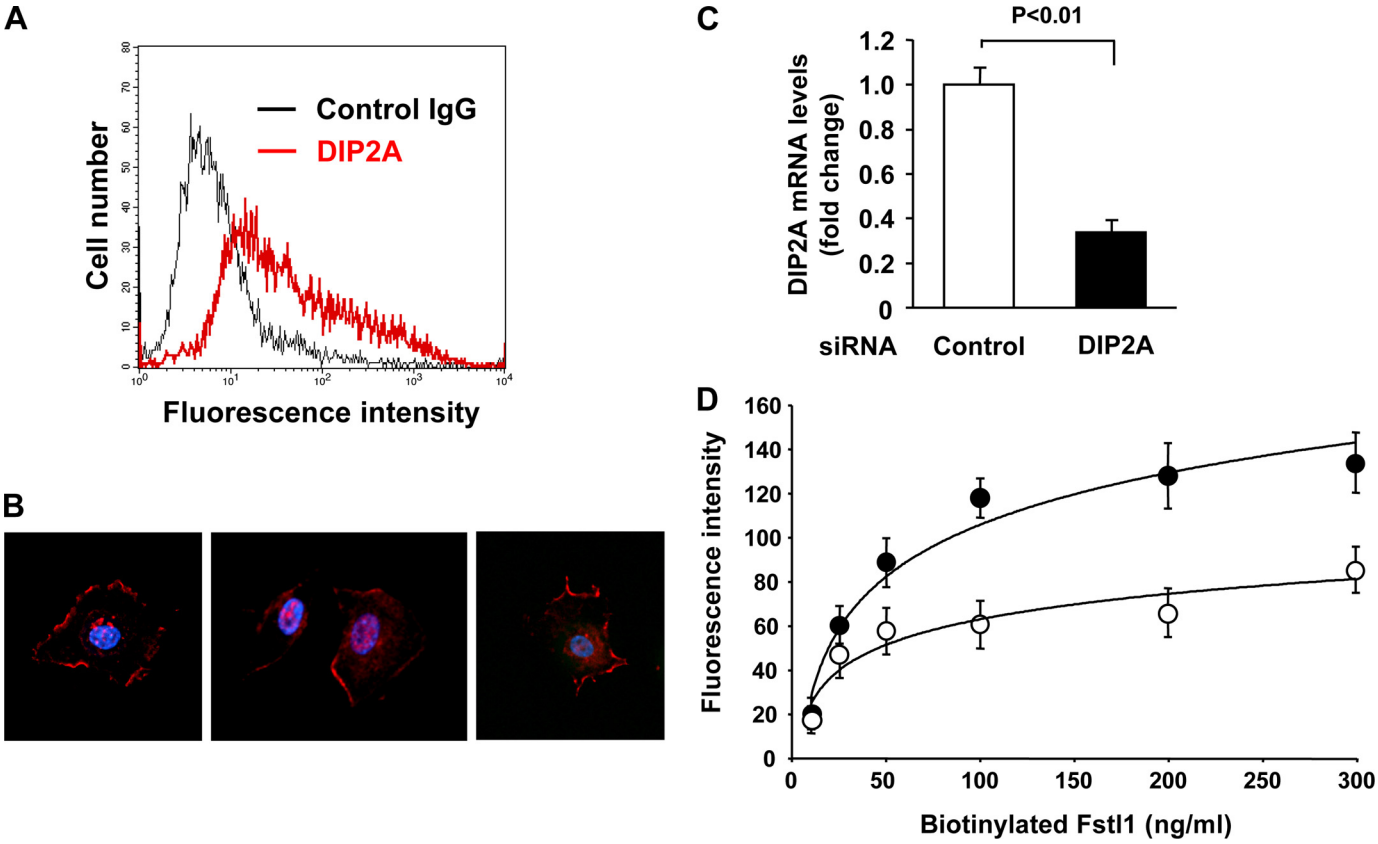

FIGURE 2. **Involvement of DIP2A in FSTL1 binding to endothelial cells.** *A*, detection of DIP2A on the cell surface of HUVECs. HUVECs were incubated with anti-DIP2A antibody (*red*; mouse IgG, 5 μg/ml) or control mouse IgG (*black*) for 60 min. Cells were stained with Alexa Fluor® 488-conjugated secondary antibody and analyzed using a FACScan. *B*, immunocytochemical analysis of HUVECs with anti-DIP2A antibody. HUVECs were incubated with anti-DIP2A antibody, followed by staining with Alexa Fluor® 594-conjugated secondary antibody (*red*). Nuclei were stained with 4′,6-diamidino-2-phenylindole (*blue*). Representative pictures are shown. *C*, reduction of DIP2A mRNA expression in HUVECs following transfection with siRNA against DIP2A. At 48 h after transfection of HUVECs with siRNA against DIP2A or control siRNA, DIP2A mRNA levels were determined by quantitative real-time PCR analysis and expressed relative to 36B4 levels ($n = 3$). *D*, effect of knockdown of DIP2A on the binding of FSTL1 to HUVECs. HUVECs were transfected with siRNA targeting DIP2A (○) or unrelated siRNA (●), incubated with increasing concentrations of biotinylated recombinant FSTL1 for 60 min, and treated with streptavidin-conjugated horseradish peroxidase, followed by incubation with QuantaBlu fluorogenic peroxidase substrate. The binding was assessed with a fluorescent microplate reader ($n = 6–7$). The data were analyzed with Microsoft Excel to generate a logarithmic trend line.

DIP2A or control siRNA, followed by treatment with or without recombinant FSTL1 protein. Treatment with recombinant FSTL1 protein resulted in a significant reduction of HUVEC death caused by serum deprivation as measured by a methanethiosulfonate-based assay (Fig. 3*A*). Transfection with siRNA against DIP2A reduced the inhibitory effects of FSTL1 protein on HUVEC death without affecting the viability of cells treated with vehicle.

To corroborate these findings, we examined the involvement of DIP2A in the survival actions conferred by adenovirus-mediated overexpression of FSTL1. After transfection with siRNA against DIP2A or control siRNA, HUVECs were treated with adenoviral vectors expressing FSTL1 (Ad-FSTL1) or β-galactosidase (Ad-β-galactosidase) as a control. Ad-FSTL1 increased FSTL1 protein levels in media from HUVECs transfected with control and DIP2A siRNAs, whereas the level of FSTL1 overexpression did not differ between cells treated with DIP2A or unrelated siRNA (data not shown). Knockdown of DIP2A reversed the decrease in cell death conferred by Ad-FSTL1 without affecting cell viability in Ad-β-galactosidase-treated cells (Fig. 3*B*).

HUVEC apoptosis induced by serum starvation was also evaluated by an enzyme-linked immunosorbent assay examining the degree of nucleosome fragmentation. The suppressive effects of Ad-FSTL1 on the extent of nucleosome fragmentation were inhibited by knockdown of DIP2A (Fig. 3*C*).

To evaluate the involvement of DIP2A in FSTL1-induced endothelial cell differentiation into vascular network-like structures, HUVECs were plated on a Matrigel matrix following transfection with siRNA targeting DIP2A. Treatment of HUVECs with recombinant FSTL1 protein led to a significant increase in cell differentiation into network structures compared with control cultures treated with vehicle (Fig. 3*D*). FSTL1-stimulated network formation was diminished by siRNA-mediated reduction of DIP2A expression (Fig. 3*D*). Similarly, knockdown of DIP2A attenuated HUVEC differentiation into network structures induced by transfection with Ad-FSTL1 (Fig. 3*E*). Transfection with siRNA against DIP2A had no effects on the basal differentiation activity of HUVECs.

The ability of endothelial cells to form networks on Matrigel is dependent upon their ability to migrate. Thus, to test whether DIP2A contributes to FSTL1-induced migratory activity, a chemotaxis assay was performed using a modified Boyden chamber assay. Ad-FSTL1 stimulated the migration of HUVECs, which was diminished by treatment with siRNA targeting DIP2A (Fig. 3*F*).

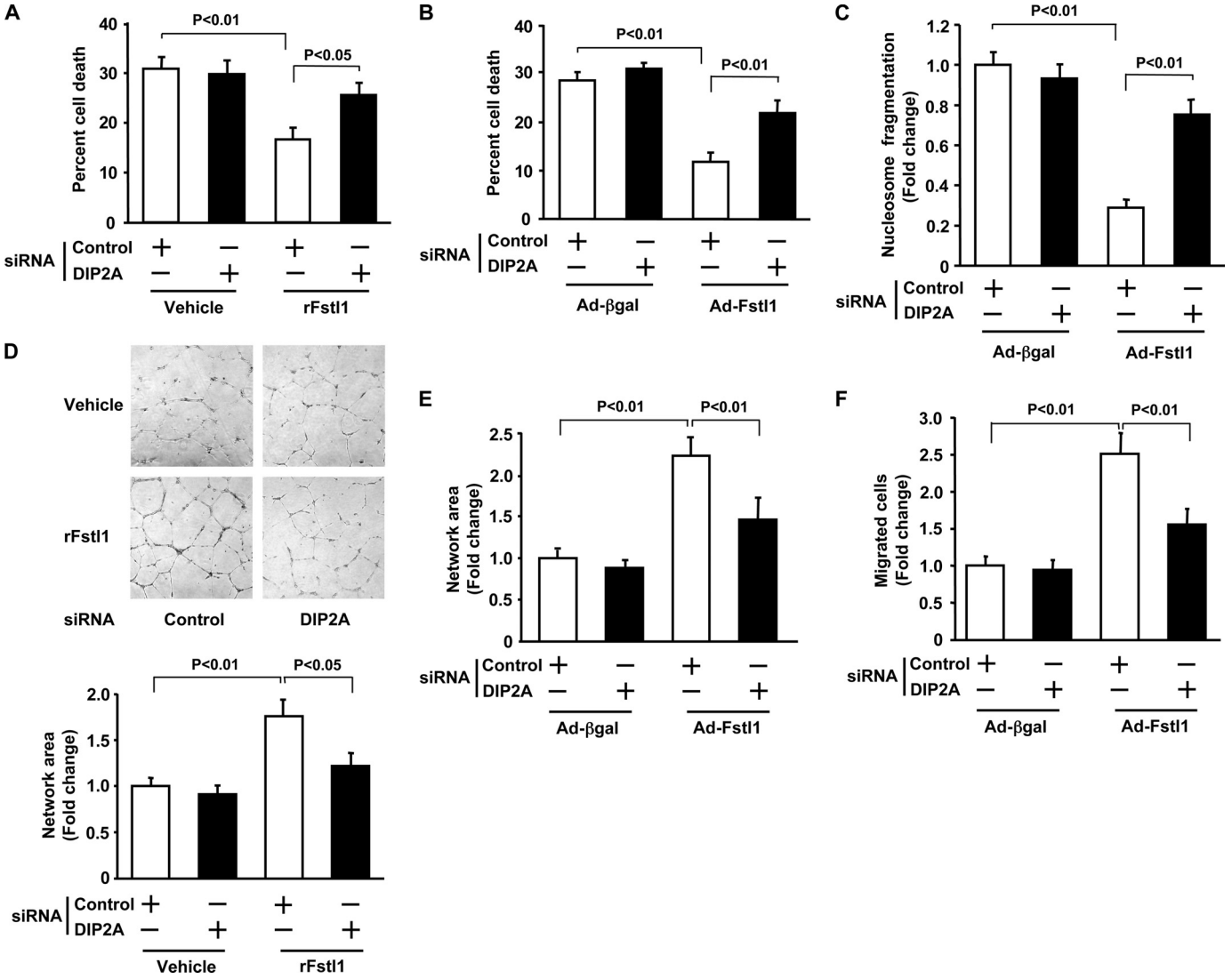

FIGURE 3. **Contribution of DIP2A to FSTL1-induced endothelial cell survival and function.** HUVECs were transduced with siRNA against DIP2A or control siRNA. *A* and *B*, effect of DIP2A deletion on FSTL1-induced inhibition of HUVEC death. *A*, HUVECs transduced with siRNA were treated with recombinant FSTL1 protein (*rFstl1*; 100 ng/ml) or vehicle in serum-free medium for 48 h. *B*, after transfection with siRNAs, HUVECs were transduced with Ad-FSTL1 or Ad-β-galactosidase (*Ad-βgal*) for 8 h, followed by incubation in serum-free medium for 48 h. HUVEC death was assessed by a quantitative methanethiosulfonate-based assay. *C*, knockdown of DIP2A blocks the inhibitory actions of FSTL1 on HUVEC apoptosis caused by serum deprivation. HUVECs were cultured as described for *B*. HUVEC apoptosis was assessed by the degree of nucleosome fragmentation. *D* and *E*, role of DIP2A in endothelial cell network formation in response to FSTL1. *D*, after siRNA transfection, HUVECs were deprived of serum for 16 h and seeded on Matrigel-coated culture dishes in the presence of recombinant FSTL1 (100 ng/ml) or vehicle. Representative cultures are shown (*upper panels*). Quantitative analyses of network formation are shown (*lower panels*). *E*, following siRNA transfection, HUVECs were transduced with Ad-FSTL1 and Ad-β-galactosidase for 8 h and incubated in serum-free medium for 16 h, followed by subjection to Matrigel matrix. Quantitative analyses of network formation are shown. *F*, DIP2A is involved in FSTL1-stimulated endothelial cell migration. HUVECs were transduced with Ad-FSTL1 and Ad-β-galactosidase for 8 h. After 24 h of serum starvation, a modified Boyden chamber assay was performed. Results are shown as means ± S.E. ($n = 4–7$). Results are expressed relative to the values compared with control siRNA with vehicle or Ad-β-galactosidase.

Involvement of DIP2A in Akt Phosphorylation in Response to FSTL1—Akt signaling is an important regulator of endothelial cell survival, migration, and differentiation into network structures (19, 20). Our recent study demonstrated that FSTL1 promotes endothelial cell function via an Akt-dependent mechanism (8). Thus, to investigate whether FSTL1 modulates Akt signaling in endothelial cells through a DIP2A-dependent pathway, HUVECs were transfected with siRNA targeting DIP2A or control sequence and incubated with FSTL1 protein or vehicle. Western blot analysis revealed that treatment with recombinant FSTL1 protein increased the activating phosphorylation of Akt at Ser^{473} in HUVECs (Fig. 4*A*). DIP2A knockdown reduced FSTL1 protein-stimulated phosphorylation of Akt without affecting basal phosphorylation (Fig. 4*A*). Likewise, knockdown of DIP2A reduced Ad-FSTL1-induced Akt phosphorylation in HUVECs (Fig. 4*B*).

DIP2A Mediates Protective Effects of FSTL1 in Cardiac Myocytes—To corroborate and extend these findings to another cardiovascular cell type, we assessed the role of DIP2A in mediating the regulatory effects of FSTL1 on cultures of NRVMs. NRVMs were transfected with siRNA targeting DIP2A or control siRNA, followed by transduction with Ad-FSTL1 or Ad-β-galactosidase. Transfection of NRVMs with siRNA against rat DIP2A decreased DIP2A mRNA expression

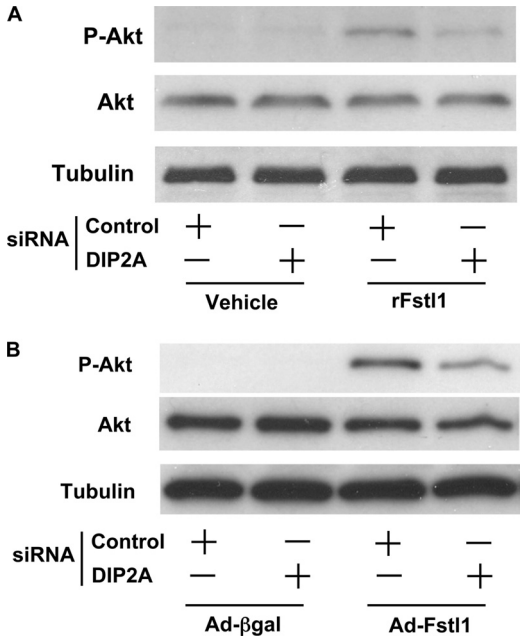

FIGURE 4. **Involvement of DIP2A in FSTL1-mediated Akt signaling.** HUVECs were transfected with siRNA against DIP2A or control siRNA. *A* and *B*, DIP2A mediates the stimulatory actions of FSTL1 on Akt phosphorylation in HUVECs. *A*, after 16 h of incubation in serum-free medium, siRNA-transfected HUVECs were treated with recombinant FSTL1 (*rFstl1*; 100 ng/ml) or vehicle for 30 min. *B*, after transfection with siRNA, HUVECs were transduced with Ad-FSTL1 and Ad-β-galactosidase for 8 h and incubated in serum-free medium for 24 h. Akt phosphorylation (*P-Akt*) levels were determined by Western blot analysis. Representative blots are shown from one of three independent experiments.

by 66.4 ± 6.1% compared with unrelated siRNA (Fig. 5*A*). Cardiomyocyte apoptosis in response to hypoxia/reoxygenation was assessed by the degree of nucleosome fragmentation as measured by enzyme-linked immunosorbent assay. Treatment with Ad-FSTL1 significantly suppressed hypoxia/reoxygenation-induced cardiomyocyte apoptosis, consistent with our previous data (7). Knockdown of DIP2A by siRNA significantly reversed the inhibitory actions of Ad-FSTL1 on apoptosis of cardiac myocytes under hypoxia/reoxygenation conditions (Fig. 5*B*).

Akt signaling promotes cardiac myocyte survival (21), and we have shown previously that FSTL1 activates Akt signaling in cultured NRVMs (7). To test whether FSTL1 controls Akt signaling in cardiac myocytes via a DIP2A-dependent pathway, NRVMs were transfected with siRNA targeting DIP2A or control sequence and transduced with Ad-FSTL1 or Ad-β-galactosidase. The siRNA-mediated reduction of DIP2A reduced FSTL1-stimulated Akt phosphorylation in NRVMs without affecting basal phosphorylation levels (Fig. 5*C*).

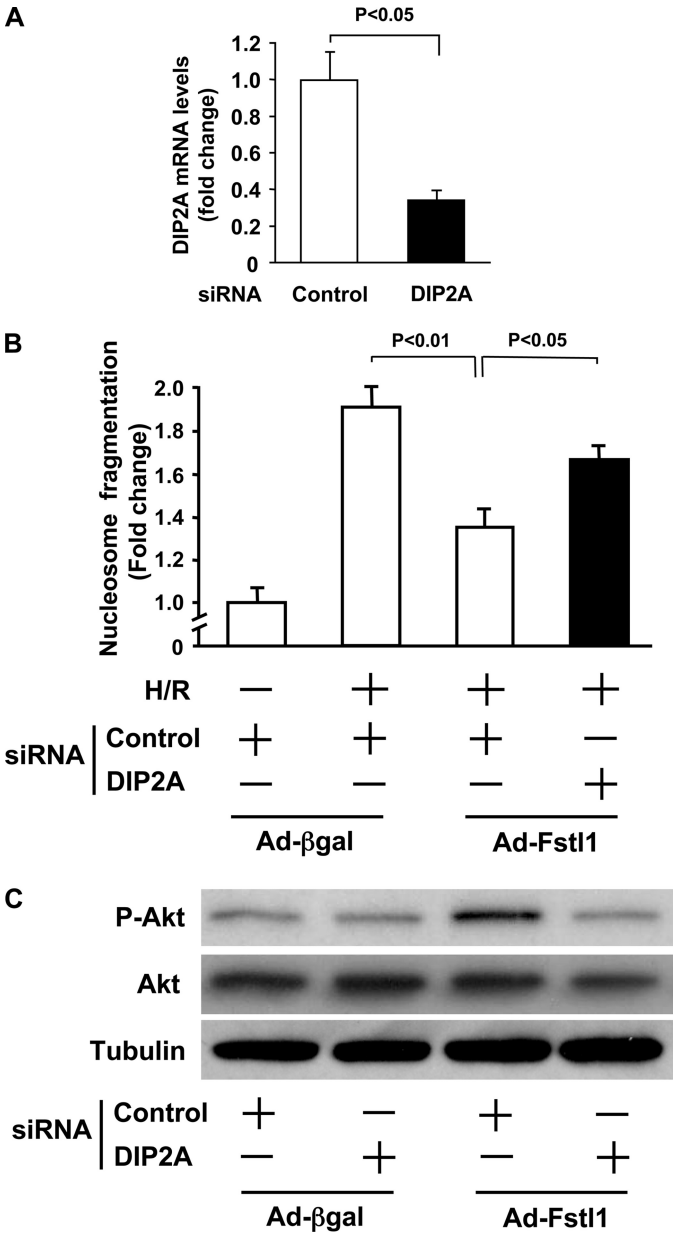

FIGURE 5. **Contribution of DIP2A to FSTL1 actions on cardiac myocytes.** NRVMs were transfected with siRNA targeting rat DIP2A or control siRNA, followed by transduction with Ad-FSTL1 and Ad-β-galactosidase (*Ad-βgal*). *A*, reduction of DIP2A mRNA expression in NRVMs transfected with siRNA against DIP2A. At 48 h after transfection of NRVMs with siRNA against DIP2A or control siRNA, DIP2A mRNA levels were measured by quantitative real-time PCR analysis and expressed relative to glyceraldehyde-3-phosphate dehydrogenase levels ($n = 3$). *B*, involvement of DIP2A in the protective effects of FSTL1 against hypoxia/reoxygenation (*H/R*)-induced NRVM apoptosis. After transfection with adenovirus, NRVMs were subjected to 12 h of hypoxia, followed by 24 h of reoxygenation. Apoptotic activity was assessed by the degree of nucleosome fragmentation. Results are shown as means ± S.E. The scale from 0 to 1.0 is minimized to highlight differences in nucleosome fragmentation values. *C*, DIP2A mediates FSTL1-induced Akt signaling in cardiac myocytes. After transduction with adenovirus, NRVMs were cultured in serum-free medium for 24 h. Akt phosphorylation (*P-Akt*) levels were determined by Western blot analysis. Representative blots are shown from one of three independent experiments.

DISCUSSION

This study provides the first evidence that FSTL1 modulates endothelial cell phenotype via a DIP2A receptor-dependent mechanism. We identified DIP2A from the membrane fraction of endothelial cells as a cell-surface binding protein of FSTL1 in a pulldown assay using FLAG-tagged FSTL1 as a bait protein. Immunoprecipitation assays provided evidence for a direct interaction between FSTL1 and DIP2A. Furthermore, gene knockdown experiments revealed that DIP2A is required for the stimulatory effects of FSTL1 on Akt activation and cell survival, differentiation, and migration. Thus, we propose that DIP2A acts as a functional receptor of FSTL1 and plays an essential role in regulation of the endothelial cell response to

FSTL1. We also found that the actions of FSTL1 on hypoxia/reoxygenation-induced apoptosis and Akt activation in cardiac myocytes are largely dependent on DIP2A. Therefore, DIP2A can mediate multiple aspects of the cardiovascular protective actions attributed to FSTL1.

DIP2 was initially identified by a yeast two-hybrid screen as a protein that interacts with a transcription factor encoded by the *Drosophila Disco* gene (22). Mutations in the *Disco* locus give rise to flies that exhibit abnormal neuronal connections in the visual system (23). No functional studies have been performed on the *Drosophila* DIP2 protein or on its vertebrate homolog DIP2A. Analysis of *Dip2* transcripts by *in situ* hybridization showed that the expression of this gene is observed in the nervous systems of *Drosophila*, and the mouse homolog is reported to be selectively expressed in the nervous system of the murine embryo (22). In contrast, in adult human tissues, the *DIP2A* transcript (also referred to as KIAA0184) is ubiquitously expressed (24).[3] The DIP2/DIP2A sequence is evolutionarily conserved from *Drosophila* to human with 50% homology at the amino acid level. Surprisingly, a vertebrate homolog of *Drosophila Disco* does not exist based upon a UniGene search. Thus, it is highly unlikely that DIP2A exerts biological actions in vertebrate cells by interacting with a Disco-like factor.

Human DIP2A is a 170-kDa protein containing DMAP1-binding, CaiC (acyl-CoA synthetase (AMP-forming)/AMP-acid ligase I), and AMP-binding enzyme domains. However, the significance of these domains in DIP2A function is not known at this time, and the NCBI Conserved Domains Program rates these assignments with low probabilities. Bioinformatic analysis of the subcellular localization by the PSORT II program demonstrated the possible presence of DIP2A in plasma membrane (43.5%). The PSORT II analysis also suggested a 39.1% probability of localization to the endoplasmic reticulum and only 8.7, 4.3, and 4.3% probabilities of localization to nuclear, secretory vesicle, and mitochondrial compartments, respectively. Consistent with localization on the plasma membrane, we could immunologically detect DIP2A on the cell surface of HUVECs by flow cytometric and microscope analyses. DIP2A was also detected in pulldown assays using FLAG-tagged FSTL1 incubated with the membrane fraction of HUVECs. Analysis of the DIP2A sequence predicts the presence of nine, seven, six, three, two, one, and zero transmembrane domains using the TMpred, PSORT II, SPLIT4, PredictProtein, SOSUI, TMMTOP2, and TMHMM2 programs, respectively. Although results from the majority of these predictive programs are consistent with the notion that DIP2A is inserted in the membrane, this lack of agreement leads to considerable uncertainty regarding the topography of this protein.

Our previous studies have shown that FSTL1 has cardiovascular protective properties. FSTL1 is induced in the heart in response to Akt-mediated hypertrophy and ischemic and pressure overload stresses (7). We have also shown that FSTL1 is up-regulated in skeletal muscle in response to hypertrophic signals and ischemic injury, both of which will stimulate blood vessel growth (8). In these studies, we have shown that FSTL1 can protect the heart from ischemia-reperfusion injury and stimulate the revascularization of ischemic muscle. Furthermore, cell culture studies indicate that FSTL1 can directly act on cardiac myocytes and endothelial cells to protect them from apoptosis through activation of the Akt protein kinase, a key regulator of growth and cell survival in the cardiovascular system (25). The work in the current study identifies DIP2A as a novel receptor for FSTL1 that mediates Akt activation and cell survival and function in cardiovascular cells *in vitro*. Thus, it will be of interest to examine the role of DIP2A in models of cardiovascular stress *in vivo*.

In addition to its cardiovascular protective functions, FSTL1 has also been implicated in immune cell regulation. Autoantibodies against FSTL1 are observed in the sera of patients with rheumatoid arthritis, and systemic delivery of FSTL1 protein is reported to ameliorate joint inflammation in a mouse model of arthritis (4). A recent study showed that *Fstl1* transcripts are up-regulated in a model of heart allograft tolerance and that adenovirus-mediated systemic administration of FSTL1 results in improved allograft survival associated with reduced expression of pro-inflammatory cytokines, including interleukin-6 and interleukin-17A (5). In contrast, adenovirus-mediated overexpression of FSTL1 in mouse paws leads to severe arthritis in association with increased production of tumor necrosis factor-α and interleukin-6 (6). Thus, it is controversial whether FSTL1 is protective or detrimental in the setting of inflammatory response, and it will be of interest to test whether the FSTL1-DIP2A axis is involved in the regulation of inflammation.

In conclusion, we have provided evidence that FSTL1 promotes changes in signaling and cell phenotype through interactions with DIP2A on the cell surface. These data suggest that the FSTL1-DIP2A signaling axis is a regulator of intertissue communication within the cardiovascular system. Further characterization of DIP2A should elucidate the physiological functions of FSTL1 in different cell types and provide a better understanding of the pathogenesis of ischemic cardiovascular diseases.

Acknowledgment—We thank Dr. Margaretha Carraway for helpful advice.

REFERENCES

1. Shibanuma, M., Mashimo, J., Mita, A., Kuroki, T., and Nose, K. (1993) *Eur. J. Biochem.* **217,** 13–19
2. Sumitomo, K., Kurisaki, A., Yamakawa, N., Tsuchida, K., Shimizu, E., Sone, S., and Sugino, H. (2000) *Cancer Lett.* **155,** 37–46
3. Chan, Q. K., Ngan, H. Y., Ip, P. P., Liu, V. W., Xue, W. C., and Cheung, A. N. (2009) *Carcinogenesis* **30,** 114–121
4. Kawabata, D., Tanaka, M., Fujii, T., Umehara, H., Fujita, Y., Yoshifuji, H., Mimori, T., and Ozaki, S. (2004) *Arthritis Rheum.* **50,** 660–668
5. Le Luduec, J. B., Condamine, T., Louvet, C., Thebault, P., Heslan, J. M., Heslan, M., Chiffoleau, E., and Cuturi, M. C. (2008) *Am. J. Transplant.* **8,** 2297–2306
6. Miyamae, T., Marinov, A. D., Sowders, D., Wilson, D. C., Devlin, J., Boudreau, R., Robbins, P., and Hirsch, R. (2006) *J. Immunol.* **177,** 4758–4762
7. Oshima, Y., Ouchi, N., Sato, K., Izumiya, Y., Pimentel, D. R., and Walsh, K. (2008) *Circulation* **117,** 3099–3108
8. Ouchi, N., Oshima, Y., Ohashi, K., Higuchi, A., Ikegami, C., Izumiya, Y., and Walsh, K. (2008) *J. Biol. Chem.* **283,** 32802–32811

[3] N. Ouchi, unpublished data.

9. Hambrock, H. O., Kaufmann, B., Müller, S., Hanisch, F. G., Nose, K., Paulsson, M., Maurer, P., and Hartmann, U. (2004) *J. Biol. Chem.* **279,** 11727–11735
10. Balemans, W., and Van Hul, W. (2002) *Dev. Biol.* **250,** 231–250
11. Mashimo, J., Maniwa, R., Sugino, H., and Nose, K. (1997) *Cancer Lett.* **113,** 213–219
12. Ouchi, N., Kobayashi, H., Kihara, S., Kumada, M., Sato, K., Inoue, T., Funahashi, T., and Walsh, K. (2004) *J. Biol. Chem.* **279,** 1304–1309
13. Ohashi, K., Ouchi, N., Sato, K., Higuchi, A., Ishikawa, T. O., Herschman, H. R., Kihara, S., and Walsh, K. (2009) *Mol. Cell. Biol.* **29,** 3487–3499
14. Pimentel, D. R., Amin, J. K., Xiao, L., Miller, T., Viereck, J., Oliver-Krasinski, J., Baliga, R., Wang, J., Siwik, D. A., Singh, K., Pagano, P., Colucci, W. S., and Sawyer, D. B. (2001) *Circ. Res.* **89,** 453–460
15. Takemura, Y., Ouchi, N., Shibata, R., Aprahamian, T., Kirber, M. T., Summer, R. S., Kihara, S., and Walsh, K. (2007) *J. Clin. Invest.* **117,** 375–386
16. Ouchi, N., Shibata, R., and Walsh, K. (2005) *Circ. Res.* **96,** 838–846
17. Kobayashi, H., Ouchi, N., Kihara, S., Walsh, K., Kumada, M., Abe, Y., Funahashi, T., and Matsuzawa, Y. (2004) *Circ. Res.* **94,** e27–e31
18. Shibata, R., Sato, K., Pimentel, D. R., Takemura, Y., Kihara, S., Ohashi, K., Funahashi, T., Ouchi, N., and Walsh, K. (2005) *Nat. Med.* **11,** 1096–1103
19. Fujio, Y., and Walsh, K. (1999) *J. Biol. Chem.* **274,** 16349–16354
20. Kureishi, Y., Luo, Z., Shiojima, I., Bialik, A., Fulton, D., Lefer, D. J., Sessa, W. C., and Walsh, K. (2000) *Nat. Med.* **6,** 1004–1010
21. Fujio, Y., Nguyen, T., Wencker, D., Kitsis, R. N., and Walsh, K. (2000) *Circulation* **101,** 660–667
22. Mukhopadhyay, M., Pelka, P., DeSousa, D., Kablar, B., Schindler, A., Rudnicki, M. A., and Campos, A. R. (2002) *Gene* **293,** 59–65
23. Steller, H., Fischbach, K. F., and Rubin, G. M. (1987) *Cell* **50,** 1139–1153
24. Nagase, T., Seki, N., Ishikawa, K., Tanaka, A., and Nomura, N. (1996) *DNA Res.* **3,** 17–24
25. Shiojima, I., and Walsh, K. (2006) *Genes Dev.* **20,** 3347–3365